The effect of cation disorder on electrical transport properties of $Nd_{0.7}(Ca, Sr, Ba)_{0.3}MnO_3$



1999 J. Phys.: Condens. Matter 11 6877

(http://iopscience.iop.org/0953-8984/11/36/305)

J. Phys.: Condens. Matter **11** (1999) 6877–6882. Printed in the UK PII: S0953-8984(99)03169-0

# The effect of cation disorder on electrical transport properties of $Nd_{0.7}(Ca, Sr, Ba)_{0.3}MnO_3$

Zhou Shengming†‡, Zhu Hong†, Shi Lei†, Zhao Zongyan‡, Zhou Guien† and Zhang Yuheng†

† Structure Research Laboratory, University of Science and Technology of China, Academia Sinica, Hefei 230026, People's Republic of China

‡ Department of Physics, Anhui University, Hefei 230039, People's Republic of China

Received 6 April 1999

**Abstract.** The electrical transport properties of a series of samples, $Nd_{0.7}(Ca, Sr, Ba)_{0.3}MnO_3$, with a fixed average A-site cation radius $\langle r_A \rangle$ have been studied. Infrared spectra revealed that the symmetry of the local $MnO_6$ octahedra reduces due to the size differences between various A-site ions. From the metal transition temperature $T_m$ up to room temperature, the variable-range-hopping conduction mechanism has been observed, and $T_m$ exhibits a systematic decrease with increasing A-site cation disorder. In the very-low-temperature range, we have observed that resistivity increases with decreasing temperature.

## 1. Introduction

Manganese perovskites are of considerable current interest owing to a colossal decrease of resistivity in an applied magnetic field near the metal–insulator transition temperature ($T_m$) that can be controlled by hole doping and the A-site cation sizes [1–5]. In the $ABO_3$ perovskite structure, the mismatch between the equilibrium bond lengths A–O and B–O is given by the deviation from unity of the tolerance factor $t = (\text{A–O})/\sqrt{2}(\text{B–O})$. For $t < 1$, the internal stresses of the lattice are relieved by a cooperative rotation of the $BO_6$ octahedra that lowers the symmetry of the unit cell from cubic to, for example, orthorhombic [1]. However, for two or more A-site species, with fractional occupancies and different cation radii, the local structure is quite distinct from that suggested by the crystallographic structure [6]. Recently, Rodriguez-Martinez and Attfield have studied the effect of this A-site cation disorder quantified by the size variance of the A-site cation-radius distribution $\sigma^2 = \langle r_A^2 \rangle - \langle r_A \rangle^2$ on the metal–insulator transition temperature $T_m$, and found that $T_m$ shows a strong linear dependence upon $\sigma^2$ ($\mathrm{d}T_m/\mathrm{d}\sigma^2 = -20\,600 \pm 500$ K Å$^{-2}$) in a series of $(L_{0.7}M_{0.3})MnO_3$ perovskites with a constant mean A-site cation radius $\langle r_A \rangle = 1.23$ Å [4, 5]. Therefore A-site cation disorder with a constant mean $\langle r_A \rangle$ shows interesting effects and is worthy of further investigation. In this paper, we focus on the effect of A-site cation disorder on electrical transport properties. We have prepared a series of six samples of $Nd_{0.7}(Ca, Sr, Ba)_{0.3}MnO_3$ (table 1), in which $\sigma^2$ is systematically varied by use of different compositions of Ca, Sr and Ba. These samples are designed to have a fixed rare-earth element (Nd), a fixed doping level ($x = 0.3$) and a fixed mean A-site radius ($\langle r_A \rangle = 1.21$ Å is calculated from tabulated values [7]) in order to ensure that the observed changes are mainly caused by A-site cation disorder. In addition, the relatively low $T_m$ of these samples can offer a wide temperature range over which we can study the electrical transport properties

0953-8984/99/366877+06$30.00  

**Table 1.** The resistivity maximum $\rho_m$, the metal–insulator transition temperature measured from the resistivity ($T_m$) and the unit-cell volume measured at room temperature with cation-size variance $\sigma^2$ for a series of $Nd_{0.7}(Ca, Sr, Ba)_{0.3}MnO_3$ perovskites with constant $\langle r_A \rangle = 1.21$ Å.

| Sample | | $\sigma^2$ (Å$^2$) | $\rho_m$ (Ω cm) | $T_m$ (K) | $V_c$ (Å$^3$) |
|---|---|---|---|---|---|
| 1 | $Nd_{0.7}Sr_{0.3}MnO_3$ | 0.0045 | 0.226 | 211 | 230.420(5) |
| 2 | $Nd_{0.7}Ca_{0.033}Sr_{0.24}Ba_{0.027}MnO_3$ | 0.0058 | 1.321 | 182 | 230.525(3) |
| 3 | $Nd_{0.7}Ca_{0.066}Sr_{0.18}Ba_{0.054}MnO_3$ | 0.0070 | 31.334 | 152 | 230.625(3) |
| 4 | $Nd_{0.7}Ca_{0.099}Sr_{0.12}Ba_{0.081}MnO_3$ | 0.0083 | 285.190 | 119 | 230.719(4) |
| 5 | $Nd_{0.7}Ca_{0.132}Sr_{0.06}Ba_{0.108}MnO_3$ | 0.0096 | 17447.300 | 84 | 230.796(5) |
| 6 | $Nd_{0.7}Ca_{0.165}Ba_{0.135}MnO_3$ | 0.0108 | — | — | 230.860(3) |

quantitatively above $T_m$. We have found that cation disorder reduces the localization length. From $T_m$ up to room temperature, the variable-range-hopping conduction mechanism has been observed. At the lowest temperatures, resistivity increases with decreasing temperature.

## 2. Experiment

The samples were prepared from stoichiometric amounts of $Nd_2O_3$, $MnO_2$, $CaCO_3$, $SrCO_3$ and $BaCO_3$ by solid-state reaction under identical conditions. After pre-sintering with three intermediate grindings in air at 1000–1200 °C for three days, the mixtures were then pressed into discs and sintered at 1420 °C for 16 h. In order to minimize micro-inhomogeneity, the sintered hard discs were broken to pieces, reground to fine powder and again pressed into discs. The final sintering was carried out in air at 1440 °C for 12 h. The samples were then slowly cooled down to room temperature. X-ray powder diffraction (XRD) analyses were performed using an MXP18AHF x-ray diffractometer with a rotating anode operating at 40 kV and 100 mA. Cu K$\alpha$ radiation was selected using a graphite monochromator. Structural parameters were refined by the Rietveld method, using the program DBWS-9411 [8]. Electrical resistivity was measured by the standard four-probe method. The measurements of infrared (IR) transmission spectra (Nicolet 700) were carried out with powder samples in which KBr is used as a carrier. The IR spectra taken are in the frequency range from 4000 to 350 cm$^{-1}$.

## 3. Results and discussion

All lines of the XRD patterns for the $Nd_{0.7}(Ca, Sr, Ba)_{0.3}MnO_3$ samples could be indexed with the *Pnma* space group (see figure 1), thus confirming that all samples were of perfect single phase with the same space group. The room temperature unit-cell volume slightly increases with increasing $\sigma^2$ (see table 1). A-site cation disorder results mainly in random displacements of oxygen atoms from their average crystallographic positions [4, 5]. Directly evidence for this can be obtained from IR spectra which are sensitive to local lattice distortions. Figure 2 depicts the observed IR spectra of the three mixed oxides with $\sigma^2 = 0.0045$, 0.0070 and 0.0108 Å$^2$ respectively. Obviously, two strong absorption regions are present for all samples. The negative peaks around $\nu = 594$ cm$^{-1}$ are assigned to the stretching vibration mode of the $MnO_6$ octahedron in which the Mn–O bond distance is modulated and the negative peaks around $\nu = 391$ cm$^{-1}$ are assigned to the bending vibration in which the Mn–O–Mn bond angle is modulated [9]. As seen in figure 2, the bending vibration becomes more prominent with increasing $\sigma^2$; this directly reflects the fact that the symmetry of the local $MnO_6$ octahedra reduces with increasing $\sigma^2$ due to random displacements of oxide ions. Therefore it can be stated that A-site cation disorder results in local distortions of $MnO_6$ octahedra which can be viewed as the

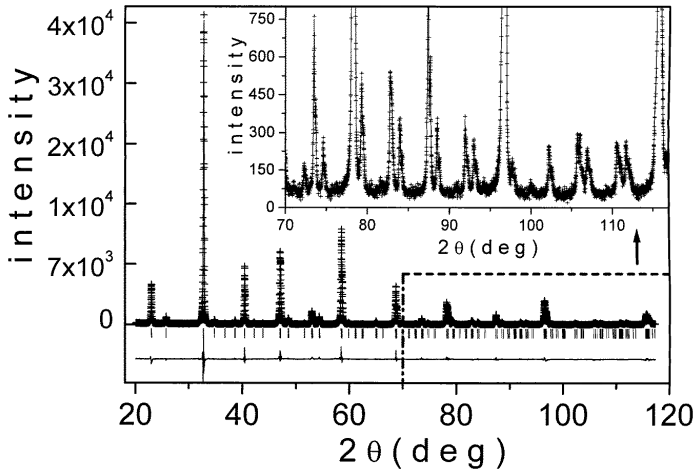


**Figure 1.** The output from the Rietveld analysis of the XRD pattern for one of the samples of $Na_{0.7}(Ca, Sr, Ba)_{0.3}MnO_3$ with $\sigma^2 = 0.0070$ Å$^2$. The plus signs show raw data. The solid line is the calculated profile. The vertical bars indicate the expected Bragg reflection positions. The lowest curve is the difference between the observed and calculated intensity, plotted on the same scale and shifted downwards a little for clarity.

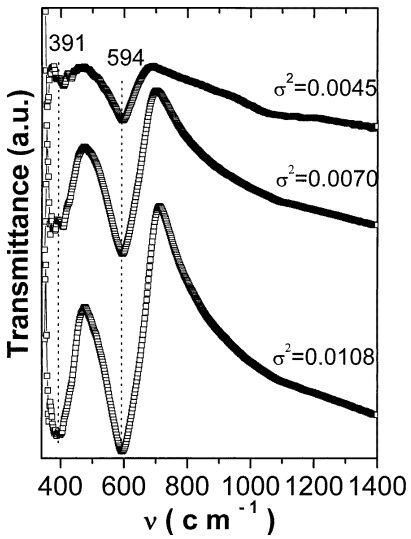


**Figure 2.** IR transmittance spectra for $Nd_{0.7}(Ca, Sr, Ba)_{0.3}MnO_3$ with $\sigma^2 = 0.0045$, 0.0070 and 0.0108 Å$^2$, at room temperature.

random impurity potential in the lattice. The temperature-dependent resistivity at zero field for the six samples is shown in figure 3. Increasing $\sigma^2$ causes a decrease in $T_m$ and an increase in the magnitude of the resistivity. Note that for $\sigma^2 = 0.0108$ Å$^2$, $\rho$ increases sharply with decreasing temperature and exceeds the experimental limit. Here, we can see that $\rho$ versus $T$ above $T_m$ is virtually identical for all the samples, the only difference being that the magnitude increases with increasing $\sigma^2$. This suggests that the natures of the charge transport in the nonmetallic

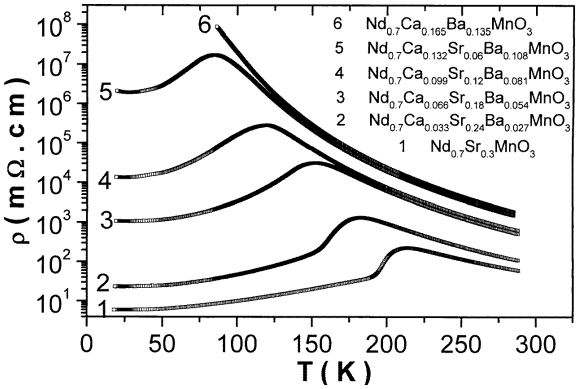


**Figure 3.** The temperature-dependent resistivity of $Nd_{0.7}(Ca, Sr, Ba)_{0.3}MnO_3$ with different A-site size variances $\sigma^2$. The samples are numbered in order of increasing $\sigma^2$.

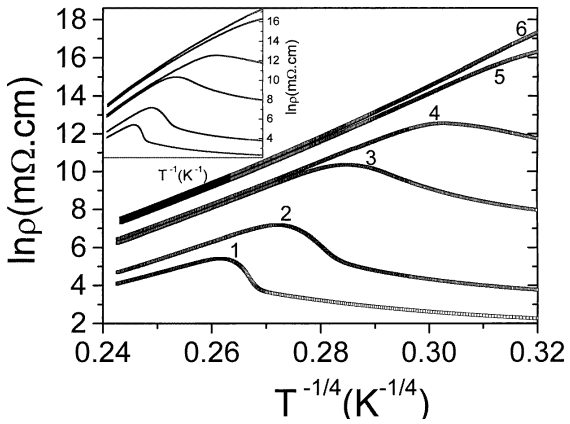


**Figure 4.** $\ln(\rho)$ is plotted against $T^{-1/4}$ for the six samples in the series $Nd_{0.7}(Ca, Sr, Ba)_{0.3}MnO_3$. The inset shows $\ln(\rho)$ versus $T^{-1}$ for the corresponding samples in the same temperature range (from room temperature down to 95 K).

state above $T_m$ are the same. At temperatures above $T_m$ and up to room temperature, $\rho(T)$ can be described better by $\rho(T) = \rho(0)\exp(T_0/T)^{1/4}$ than by $\rho(T) = \rho(0)\exp(E_0/k_BT)$; the former is typically found when conduction takes place by hopping between localized states (variable-range hopping) [10]. A relatively good fit is obtained for all of the samples and it is also clear from the linear behaviour of the plot of $\ln\rho$ versus $T^{-1/4}$ as shown in figure 4 ($\ln\rho$ versus $T^{-1}$ is also plotted in the inset for comparison). The values of $T_0$ obtained from this fitting are increasing with $\sigma^2$ as shown in figure 5, where systematic change of $T_0$ and $T_m$ with $\sigma^2$ is observed. In the theory of variable-range hopping, the $T_0$-parameter is related to the decay length ($L$) of the localized wave function and to the density of states ($g(E_F)$) at the Fermi level: $T_0 \propto 1/L^3 g(E_F)$. The bandwidth is calculated from the average bond distances and angles; for the $Nd_{0.7}(Ca, Sr, Ba)_{0.3}MnO_3$ series with fixed doping and constant $\langle r_A \rangle$, the changes in bandwidth and $g(E_F)$ are very small [5], so one can expect $L$ to decrease with increasing $\sigma^2$. Thus we obtained that increasing $\sigma^2$ associated with increasing the lattice distortions decreases the localization length $L$ and consequently the carrier mobility is reduced. $T_m$ shows a strong lin-

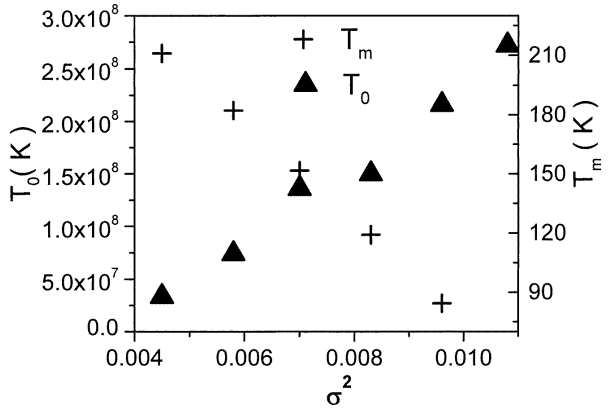


**Figure 5.** $T_0$ and $T_m$ are plotted against $\sigma^2$.

ear dependence upon $\sigma^2$, which is consistent with the results obtained by Rodriguez-Martinez and Attfield [4]. For their series of samples with $\langle r_A \rangle = 1.23$ Å, the experimental value of $dT_m/d\sigma^2$ is $-20\,600 \pm 500$ K Å$^{-2}$. But for the present series of samples with $\langle r_A \rangle = 1.21$ Å, $dT_m/d\sigma^2 = -24\,907 \pm 472$ K Å$^{-2}$. Here we can see that $dT_m/d\sigma^2$ is strongly dependent on $\langle r_A \rangle$. With increasing $\sigma^2$ (increasing localization of carriers), the reduced carrier itineracy suppresses the double-exchange interaction and hence $T_m$. According to the results in the literature [1, 3, 4] and the present study, at fixed doping level, both $\langle r_A \rangle$ and $\sigma^2$ are key factors for determining the temperature at which ferromagnetic ordering occurs. At very low temperatures, all of the samples have shown minima in the resistivity and at even lower temperature, there is a small rise in the resistivity down to the lowest temperature measured. The resistivity minimum occurs in the metallic phase in the temperature range below 30 K. As shown in figure 6, the temperature of the minima seems to increase with increasing $\sigma^2$; this implies that such low-temperature resistivity behaviour is intimately related to A-site cation disorder. A similar phenomenon of the appearance of a minimum has also been observed for other manganite samples in a similar temperature range [11, 12]. The gradual increase in $\rho(T)$ with decreasing $T$ below 24 K may reflect lowering numbers of phonons coupling to the electrons [11].

As shown in figures 3 and 6, the zero-field residual resistivity $\rho_0$ increases dramatically with increasing $\sigma^2$. According to the result obtained by Rodriguez-Martinez and Attfield that the mean ferromagnetically ordered moments at the Mn site at 4 K are close to the ideal value of 3.7 $\mu_B$ and show no significant variation with $\sigma^2$ in a series of $(L_{0.7}M_{0.3})MnO_3$ perovskites [5], the possibility that spin-disorder scattering increases with increasing $\sigma^2$ at lowest temperatures can be ruled out. Therefore $\rho_0$ originates mainly from the random impurity potential which can lower the mobility of carriers and increase the number of trapped carriers. The less-itinerant carriers at lowest temperatures seem not to contribute to the macroscopic charge transport, but can still mediate the ferromagnetic double-exchange interaction in a bond-percolative manner. This idea was presented previously to explain why an insulating but ferromagnetic state exists near the insulator-to-metal phase boundary for $La_{1-x}Sr_xMnO_3$ [2].

In summary, the infrared spectra measurements confirm that increasing A-site cation-size variance $\sigma^2$ results in increasing local distortions of $MnO_6$ octahedra in the orthomanganites $Nd_{0.7}(Ca, Sr, Ba)_{0.3}MnO_3$ with a constant average A-site cation radius $\langle r_A \rangle = 1.21$ Å. Such local structure distortions can be thought of as introducing the random impurity scattering potential and greatly increasing the resistivity and decreasing the metal–insulator transition

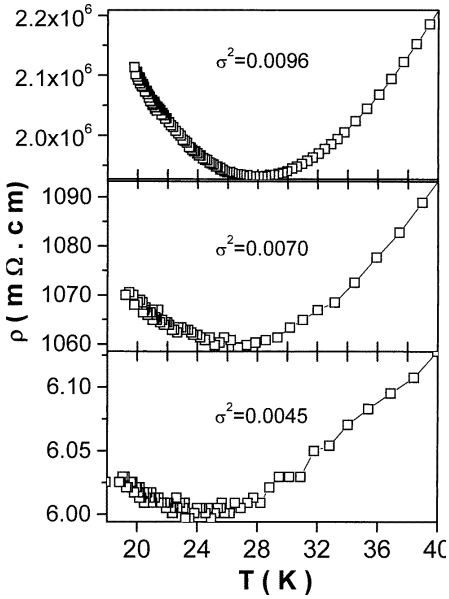


**Figure 6.** Expanded resistivity data for three samples in the series $Nd_{0.7}(Ca, Sr, Ba)_{0.3}MnO_3$ for $T \leqslant 40$ K.

temperature. $T_m$ shows strong linear dependence on $\sigma^2$ consistent with the results obtained by Rodriguez-Martinez and Attfield [4]. From $T_m$ up to room temperature, the observed conduction behaviours can be explained well by the variable-range-hopping mechanism. The localization length reduces with increasing A-site cation disorder. In addition, at very low temperatures, we have observed a minimum in the resistivity; this phenomenon seems to be related to A-site cation disorder.

## Acknowledgments

This work was financially supported by the Foundation of the Academia Sinica and by the Education and Science Committee of Anhui Province, People's Republic of China.

## References

[1] Hwang H Y, Cheong S-W, Radaelli P G, Marezio M and Batlogg B 1995 *Phys. Rev. Lett.* **75** 914
[2] Urushibara A, Moritomo Y, Arima T, Asamitsu A, Kido G and Tokura Y 1995 *Phys. Rev.* B **51** 14 103
[3] Fontcuberta J, Martínez B, Seffar A, Piñol S, García-Muñoz J L and Obradors X 1996 *Phys. Rev. Lett.* **76** 1122
[4] Rodriguez-Martinez L M and Attfield J P 1996 *Phys. Rev.* B **54** R15 622
[5] Rodriguez-Martinez L M and Attfield J P 1998 *Phys. Rev.* B **58** 2426
[6] Louca D, Egami T, Brosha E L, Röder H and Bishop A R 1997 *Phys. Rev.* B **56** R8475
[7] Shannon R D 1976 *Acta Crystallogr.* A **32** 751
[8] Young R A, Sakthivel A, Moss T S and Paiva-Santos C O 1995 *J. Appl. Crystallogr.* **28** 366
[9] Tajima S, Masaki A, Uchida S, Matsuura T, Fueki K and Sugai S 1987 *J. Phys. C: Solid State Phys.* **20** 3469
[10] Mott N F and Davis E A 1971 *Electronic Processes in Non-Crystalline Materials* (Oxford: Oxford University Press)
[11] Zhou J S, Archibald W and Goodenough J B 1996 *Nature* **381** 770
[12] Barman A, Ghosh M, Biswas S, De S K and Chatterjee S 1998 *Solid State Commun.* **106** 691